Development of sensitivity to global form and motion in macaque monkeys (*Macaca nemestrina*)

Lynne Kiorpes *, Tracy Price, Cynthia Hall-Haro, J. Anthony Movshon

Center for Neural Science, New York University, USA

ABSTRACT

To explore the relative development of the dorsal and ventral extrastriate processing streams, we studied the development of sensitivity to form and motion in macaque monkeys (*Macaca nemestrina*). We used Glass patterns and random dot kinematograms (RDK) to assay ventral and dorsal stream function, respectively. We tested 24 animals, longitudinally or cross-sectionally, between the ages of 5 weeks and 3 years. Each animal was tested with Glass patterns and RDK stimuli with each of two pattern types – circular and linear – at each age using a two alternative forced-choice task. We measured coherence threshold for discrimination of the global form or motion pattern from an incoherent control stimulus. Sensitivity to global motion appeared earlier than to global form and was higher at all ages, but performance approached adult levels at similar ages. Infants were most sensitive to large spatial scale (Δx) and fast speeds; sensitivity to fine scale and slow speeds developed more slowly independently of pattern type. Within the motion domain, pattern type had little effect on overall performance. However, within the form domain, sensitivity for linear Glass patterns was substantially poorer than that for concentric patterns. Our data show comparatively early onset for global motion integration ability, perhaps reflecting early development of the dorsal stream. However, both pathways mature over long time courses reaching adult levels between 2 and 3 years after birth.

© 2012 Elsevier Ltd. All rights reserved.

1. Introduction

Vision is comparatively poor in infant primates and develops over the early weeks, months, and years after birth. Different visual functions develop with different time courses. Acuity and contrast sensitivity develop similarly in human and non-human primates, reaching adult levels between 3 and 7 years in humans, and between 9 and 12 months in monkeys (Boothe et al., 1988; Ellemberg et al., 1999; Kiorpes, 1992, 2008; Teller, 1997). Temporal vision develops comparatively quickly. Stavros and Kiorpes (2008) described the time course of temporal contrast sensitivity development in monkeys and found that adult levels are reached by about 6 months after birth, substantially earlier than spatial contrast sensitivity. Similarly, Ellemberg et al. (1999) reported that temporal contrast sensitivity in human children reaches adult levels before spatial contrast sensitivity.

More complex visual functions, which may depend on the maturation of areas in extrastriate cortex, have also been studied developmentally. For example, contour integration ability develops quite late compared to spatial contrast sensitivity. Kovács and

colleagues showed that children under about age 3 could not identify a coherent contour defined by a circular ring of Gabor patches imbedded in noise, and the ability to perform the task improved well into the teenage years (Kovács, 2000; Kovács et al., 1999; but see also, Gerhardstein et al., 2004). This ability is late to develop in monkeys as well, with a failure of contour integration ability prior to about 16 weeks and development to adult levels over at least the succeeding year (Kiorpes & Bassin, 2003). The neural processes underlying contour integration are a matter of some debate, but the ability to extract a coherent percept from signals imbedded in noise appears to involves higher occipitotemporal areas as well as early retinotopic ones (Altmann, Bülthoff, & Kourtzi, 2003; Kourtzi et al., 2003; Li, Piëch, & Gilbert, 2006, 2008).

Contour integration requires the ability to process local orientation cues and then to organize coherent elements into a global texture or shape. A number of prior studies, using behavioral or evoked potential (VEP) measures, have documented sensitivity to texture boundaries and orientation cues by about 5 months of age in humans (Atkinson & Braddick, 1992; Norcia et al., 2005; Palomares et al., 2010; Sireteanu & Rieth, 1992). Sensitivity to texture-defined form also develops comparatively early in nonhuman primates (El-Shamayleh, Movshon, & Kiorpes, 2010). However, the appreciation of *global* structure in textured displays appears to require additional maturation, since VEP correlates of

---

* Corresponding author. Address: Center for Neural Science, 4 Washington Pl., Room 809, New York, NY 10003, USA.

  E-mail address: lynne@cns.nyu.edu (L. Kiorpes).

global organization become evident after 6 months (Arcand et al., 2007; Norcia et al., 2005; Pei, Pettet, & Norcia, 2007). It remains unclear why these global visual functions are slow to develop, but extrastriate areas such as V4 may play a role in limiting developmental progress (De Weerd, Desimone, & Ungerleider, 1996; Huxlin et al., 2000; Larsson, Landy, & Heeger, 2006; Merigan, 2000; Ostwald et al., 2008).

One visual function that is well accepted to depend on extrastriate cortical processing is motion integration. The percept of coherent motion in random dot kinematograms (RDKs) has been strongly linked to the function of neurons in area MT/V5 (Britten et al., 1992; Newsome & Paré, 1988). Kiorpes and Movshon (2004) studied global motion sensitivity in monkeys ranging in age from birth to 3 years. Unlike contour integration tasks, monkeys were able to perform the motion direction discrimination at the earliest test ages (3–5 weeks). However, development continued over a long time course, up to 3 years. Human infants are first sensitive to directional motion cues at around 2 months after birth (see Braddick, Atkinson, & Wattam-Bell, 2003). There are few data available between infancy and about age 3, when Parrish and colleagues reported coherent motion sensitivity to be adult-like (Parrish et al., 2005). On the other hand, it seems that some aspects of motion perception are immature up to age 7 years or more (Ellemberg et al., 2003; Giaschi & Regan, 1997; Gunn et al., 2002; Parrish et al., 2005), and even beyond the first decade into adolescence (Bucher et al., 2006). Together, these data suggest a long developmental program for the extrastriate cortical areas involved in global motion perception, which may begin earlier than for form-dependent tasks.

Global form and motion sensitivity are believed to reflect the function of the ventral and dorsal extrastriate visual pathways, respectively (Ungerleider & Pasternak, 2004). The relative development of these pathways is a matter of ongoing debate. A number of investigators have argued for later onset and more extended development of the motion pathway compared to the form pathway (see Braddick, Atkinson, & Wattam-Bell, 2003; Bucher et al., 2006). Braddick et al. (2005) tested sensitivity to orientation and motion cues in infants. They showed that VEP correlates of orientation reversal were evident as early as 4 weeks in humans, while correlates of motion reversal were not evident before 7 weeks. In older children, aged 4–11 years, Gunn et al. (2002) reported that global form sensitivity reached adult levels by 10 years while motion coherence sensitivity was still somewhat poorer than in adults. However, using a static global texture pattern to tap the development of the ventral, form pathway and a random dot motion pattern to track the development of the dorsal, motion pathway in infants, Braddick, Atkinson, and Wattam-Bell (2003) reported a later onset for global form discrimination than for global motion discrimination. Similarly, other studies have shown earlier – rather than later – maturation of global motion sensitivity compared to global form. For example, Parrish et al. (2005) studied the development of global motion and texture-defined form sensitivity in the same group of children using several different metrics. They found no significant improvement in global motion sensitivity, as measured by coherence threshold, between age 3 years and adult, although other metrics of motion sensitivity continued to mature up to age 7. Their results for form sensitivity showed continued maturation up to age 10–11 years. These different results across and within studies may be due to the type of stimuli or the measure used since the age at maturation, even within a domain, depended on the exact measure used (Parrish et al., 2005). Whatever the explanation, there is no clear consensus on the relative developmental profiles for these pathways in human infants and children.

We have now tracked the development of sensitivity to global form and motion in individual macaques, measuring coherence thresholds for related classes of form and motion stimuli. We used Glass patterns (Glass, 1969) to measure global form sensitivity, and RDKs to measure global motion sensitivity. In these stimuli, the global structure is perceptible only by integration of signals across space or space–time. We tested individual macaque monkeys with both types of stimuli at multiple ages from infancy to adulthood. Sensitivity to coherent motion in RDKs was measurable earlier than sensitivity to Glass patterns and was higher at all ages, but adult performance on both tasks was reached at a similar age, 2–3 years. Our results suggest that when measured with well-matched tasks, development proceeds in parallel for these stimuli, and by inference, in the dorsal and ventral extrastriate visual pathways.

2. Materials and methods

2.1. Subjects

Twenty-four visually normal pigtail macaque monkeys (*Macaca nemestrina*), ranging in age from 5 weeks to 3 years, participated in this study. Nineteen monkeys were tested at multiple ages; the others were tested at only one age. The monkeys were born either at the Washington National Primate Research Center (Seattle, WN) or at New York University. They were hand-reared in the nursery facility of the Visual Neuroscience Laboratory at New York University. The home cage environment was enriched with food treats and toys; regular interaction with peers and humans was provided. Experimental procedures and animal care were in accordance with the NIH Guide for the Care and Use of Laboratory Animals and the guidelines of the Society for Neuroscience, and were approved by the New York University Animal Care and Use Committee.

2.2. Stimuli

Stimuli were presented on a 21″ Nanao T660i monitor subtending 32 deg at 50 cm, the viewing distance used for the youngest infants. Viewing distance was increased to 100 cm for older animals, where the monitor subtended 16 deg. The viewing distance was shorter for infants because they were tested with our reinforced-looking paradigm (see Section 2.3). Pixel size was 2.68′ at 50 cm, and 1.34′ at 100 cm. The stimuli were presented in circular patches subtending 11.4 deg at 50 cm and 5.7 deg at 100 cm. On each trial, two patches were presented simultaneously, one on the left and one on right side of the monitor; the center-to-center distance between the patches was 15.4 deg at 50 cm, and 7.7 deg at 100 cm. One patch contained either a coherent form or motion stimulus; the other contained an incoherent control stimulus (see below). The background luminance was 0.3 cd/m^2, and the dot luminance was 112 cd/m^2. Stimulus presentation was controlled by a Dell computer via a VSG2/3 video card (Cambridge Research Systems); the frame rate was 100 Hz.

The motion stimuli were random dot kinematograms (RDKs) similar to those described previously (Kiorpes & Movshon, 2004). Each video frame contained a fixed number of dots that changed position from frame to frame. Any given dot at time t appeared at a location (x, y). At time $t + \Delta t$, with a probability defined by the *coherence*, the dot reappeared at location $(x + \Delta x, y)$. If a signal dot did not reappear because $x + \Delta x$ would plot the dot outside the viewable aperture, then it was replaced by a new dot on the opposite side of the window. Incoherent dots that disappeared were replaced by new dots at random locations. The total number of dots was the same on each frame: 52 dots/frame for infants (25 dots/deg^2/s); 42 dots/frame for older monkeys (82 dots/deg^2/s). Dot diameter was typically 3 pixels (4–8′, depending on viewing distance). Δt was 20 ms. We used two types of motion at each age:

Motion detection
(RDK)

Rotational

Translational

Form detection
(Glass pattern)

Concentric

Linear
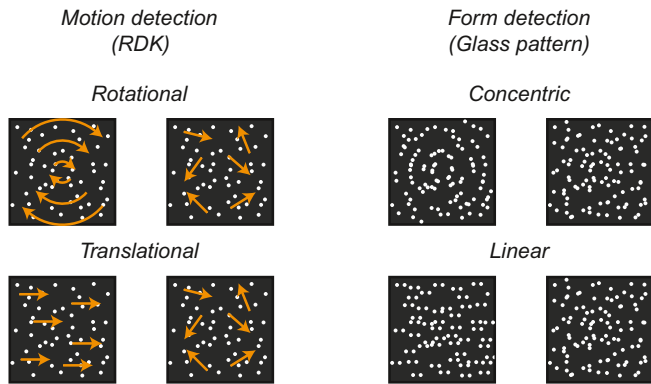
Fig. 1. Schematic representations of the stimuli. On each trial the animal saw a pair of stimuli, one of which was a coherent pattern and one of which was an incoherent control. Schematic representations of the four pattern types, two motion and two form, are illustrated. In each example pair, the coherent stimulus is on the left. Note that the actual apertures were circular.

translational motion (horizontal displacement across frames), which was randomly either rightward or leftward, and rotational motion, which was randomly either clockwise or counterclockwise (Fig. 1). The coherence level determined the strength of the global motion signal. Coherence is the proportion of dots that carry the motion signal on each frame; the probability of a dot being designated as coherent was independent from dot to dot and from frame to frame. Therefore, the direction of coherent motion could not be gleaned by following any particular dot or subset of dots; it was necessary to integrate over space and time to extract the motion signal. The speed of coherent motion was specified by $\Delta x / \Delta t$; the range of dot speed for this study was 2.2 deg/s to 26.6 deg/s. The incoherent dots provided a masking background motion with an essentially uniform distribution of directions and speeds. The incoherent control stimulus was identical except that all dots were placed randomly on each frame, yielding a percept of swirling incoherent motion. In principle, this control stimulus could be discriminated from one containing coherent motion by measuring the concentration of the spatiotemporal power spectrum of the stimulus (Britten et al., 1993). In practice, this cue is not seen and human observers can only discriminate patterns containing motion from random ones when their direction is seen (Downing & Movshon, 1989, ARVO).

Glass patterns are composed of oriented dot pairs (dipoles) presented together. They are generated by adding an exact copy of a base random dot pattern to itself following a geometric transformation such as rotation or translation (Glass, 1969; Glass & Perez, 1973). A global percept of structure is produced by the relative orientation of paired dots (dipoles) formed by integration of the dipole orientations over a large area (Fig. 1). Static Glass patterns of two types, concentric and linear, were generated as a mixture of signal and noise dipoles; the mixture on each trial was specified by pattern coherence. Each pattern contained 1024 dipoles; each dot was typically 2×2 pixels. The spatial separation between members of a dot pair was specified by Δx. The orientation of the signal dipoles was determined by the geometric transformation. The proportion of dipoles in the pattern that conformed to the geometric transformation determined its coherence. The orientation of noise dipoles was random. The separation (Δx) between members of a dot pair was the same whether it was a signal or noise dipole. We used these "random dipole" stimuli as controls because in Glass patterns, unlike RDKs as noted above, they can be distinguished from purely random ones under conditions like ours in which Δx is small compared to the distribution of interdot distances in random arrays of the same average density (Alliston, 2004). Fresh examples of all patterns were used on every trial.

The strength of the form and motion signals in our patterns is defined by a coherence parameter; as noted above, the meaning of coherence for Glass patterns and RDKs is somewhat different. In particular, at high coherence RDKs enter a regime in which long motion streaks can occur, a situation for which no Glass-pattern analogue exists. This might have the effect of enhancing the effectiveness of high-coherence motion, but not for coherences below roughly 0.25. At a coherence of 0.25, for example, the probability of a 3-element dot streak is 0.25^2, or 0.063; a four-element streak is extremely rare ($p = 0.25^3$, or 0.016). The maximum coherence value we used for RDKs was 0.8.

2.3. Psychophysical methods

Behavioral methods were similar to those described elsewhere (Hall-Haro & Kiorpes, 2008; Kiorpes & Movshon, 2004). All subjects were tested binocularly in a darkened room using a spatial two-alternative forced choice (2AFC) procedure. Monkeys were either sitting in a standard primate chair (those older than about age 2) or freely roaming in a large testing cage. Trials started when the monkey put its face into a facemask mounted on the cage or chair, which served to control the viewing distance. The presence of the face in the mask signaled the computer to present the stimuli: two apertures, one containing a coherent form or motion stimulus and one containing an incoherent control. The animals were trained to detect the one containing the coherent motion or Glass pattern stimulus. For animals under 20 weeks, we used a combination of preferential looking and operant conditioning techniques that we call "reinforced looking" (Kiorpes & Kiper, 1996; Kiorpes & Movshon, 1998; Stavros & Kiorpes, 2008). For reinforced looking, infants were trained to make an eye movement toward the side of the screen that displayed the target stimulus patch. A human observer, blind to the experimental display, judged the monkey's choice based on the animal's looking behavior. The 50 cm viewing distance ensured that the stimuli were placed far enough apart so that looks to the right and left aperture were clearly discriminable by the human observer. Older animals, were tested at the standard – 1 m – viewing distance, and indicated their own choice by pulling the appropriate one of two available grab bars mounted on the front of the cage or chair. The side containing the target stimulus was randomized from trial to trial. Stimuli were presented for up to 3 s for monkeys younger than 20 weeks and for 1 s for older monkeys. We tested three animals using both methods at the transition age to confirm that the data did not differ systematically across methods. Animals were rewarded with infant formula or apple juice, according to age, for correct responses while errors were signaled by an 1 kHz tone. Auditory masking noise was provided by a noise generator or a radio to reduce distractions from extraneous noises in the testing area.

We measured coherence threshold by varying the strength of the motion/form signal across trials using the method of constant stimuli. We measured thresholds for each animal at each age with each pattern type for both form and motion stimuli. In other words, we tested four conditions at each age: rotational and translational motion, and concentric and linear form. Each condition was tested over consecutive blocks of trials and sessions, so that, for example, all rotational motion data were collected over consecutive sessions and then translational motion was tested. The test order was randomized across conditions and animals. We fit psychometric functions, based on 3–5 coherence levels, and at least 75 trials per level, for each of a range of Δx values for each condition. Data collection was counterbalanced across Δx within a pattern type. Threshold estimates (75% correct) and associated standard errors were calculated using Probit analysis (Finney, 1971) of the log-transformed data sets. We took motion/form sensitivity to be the inverse of coherence at threshold.

To capture the developmental trajectories for different pattern types, at each age we identified the Δx value yielding the highest sensitivity, and then fit a Michaelis–Menten function to these peak values:

$$S = S_{max}\left[\frac{A^e}{A^e + C^e}\right]$$

where S is the fit sensitivity, S_{max} is the peak sensitivity, A is the subjects' age in weeks, C is the criterion age at which sensitivity reached half its maximum value, and e is the fit exponent. For cases where the model fit did not reach a clear plateau, we computed an analogous quantity for C that was restricted to be within the range of the observed data. To compute confidence intervals for these fits, we bootstrapped the data over 1000 iterations. For each of the four pattern types (translational and rotational motion; concentric and linear form), we resampled the data points with replacement, fitting the data on each iteration and extracting the parameter C (half-max age). From this analysis, we then calculated the 68% confidence intervals (±1 standard deviation) of the bootstrap estimates. To evaluate the significance of differences between two data sets, we drew 1000 estimates of C from each, and used the distributions of these estimates to compute the probability that differences as large as those observed between the values for different stimulus types could have occurred by chance. We used a similar method to compare coherence sensitivity for different pattern and motion types at the end of our developmental trajectory.

3. Results

We used a combination of longitudinal and cross-sectional testing to gather data on the relative development of motion and form sensitivity.

Longitudinal data for all four test conditions from one monkey are shown in Fig. 2. Coherence sensitivity (the inverse of threshold) is plotted as a function of dot displacement (Δx) for each of the four test conditions: rotational and translational motion, and concentric and linear form, at three ages. A number of general, representative features of the data are evident. First, at the youngest test age, 10–11 weeks, FS was able to discriminate both types of motion
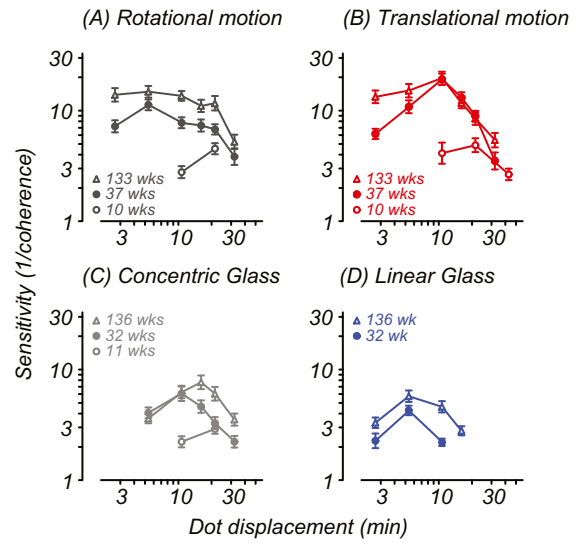
Fig. 2. Longitudinal development of sensitivity to RDK motion and Glass patterns. Coherence sensitivity is plotted as a function of dot displacement (Δx) for an individual monkey at several test ages. Data for translational and rotational motion (panels A and B) show earlier and more substantial developmental change than linear and concentric Glass patterns (panels C and D). Ages at test are indicated by symbol type; colors represent pattern type. (For interpretation of the references to color in this figure legend, the reader is referred to the web version of this article.)

(panels A and B), and could detect the structure in the concentric Glass pattern (panel C). She was unable to perform better than chance with the linear Glass patterns (panel D) at any dot displacement even with the highest coherence level (90%). FS was one of only three monkeys, out of seven tested around this age, for which we were able to establish a threshold with either type of Glass pattern; all animals were able to perform both types of motion discrimination at this age. By 15 weeks, 50% of the monkeys tested were able to detect the structure in concentric Glass patterns but only one was able to discriminate linear patterns in that age range. Second, at the youngest age, FS could perform the discriminations
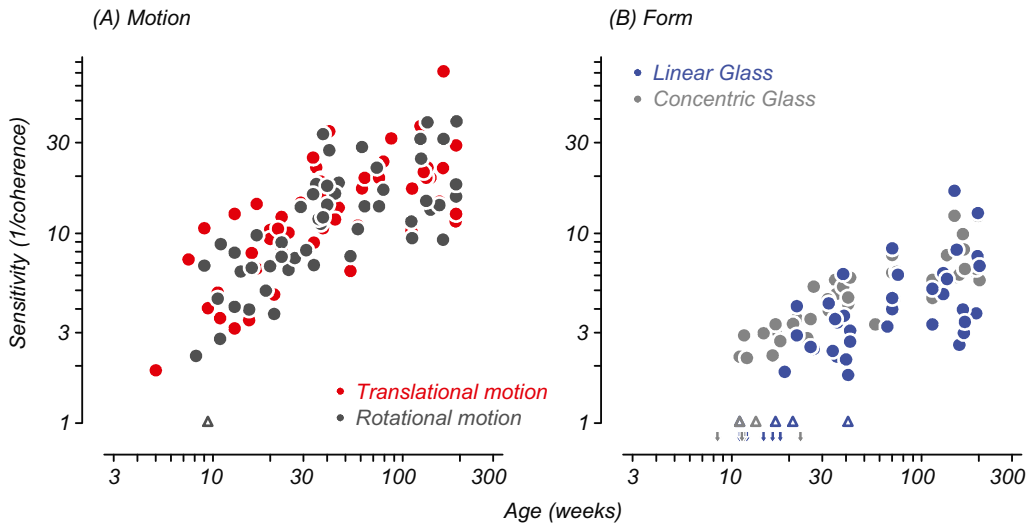
Fig. 3. Development of coherence sensitivity for all four pattern types. Coherence sensitivity is plotted as a function of age for each RDK and Glass pattern type. Rotational and translational motion sensitivity are plotted together in panel A; concentric and linear Glass pattern sensitivity are plotted together in panel B. The data points are the best sensitivity measured at each age from each monkey tested, independently of spatial scale (Δx). The small upright triangles represent cases in which the animal could discriminate the pattern (denoted by the color) from the control only at the highest coherence, so that a full psychometric function could not be measured. The arrows pointing to the abscissa represent cases in which an animal was unable to discriminate the pattern (denoted by color) from the control at any coherence or spatial scale.
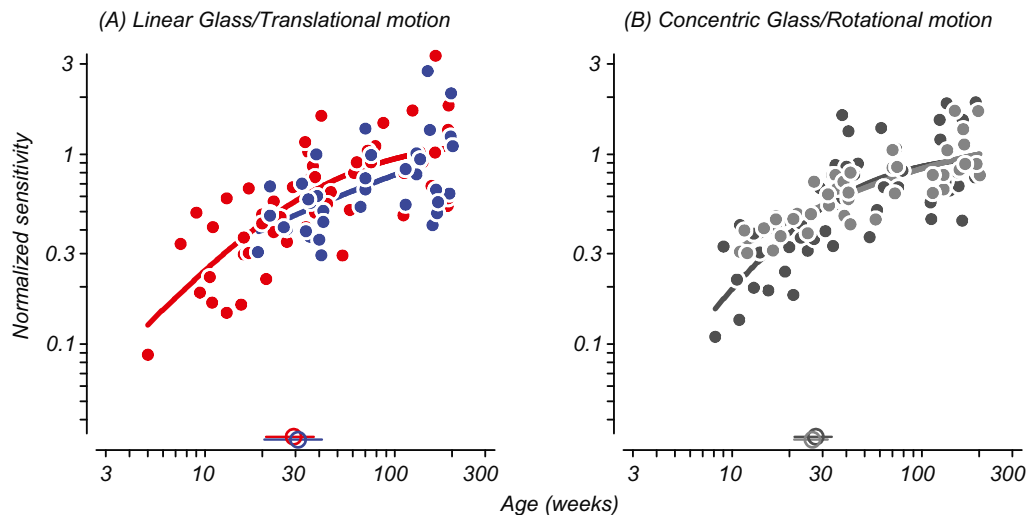
Fig. 4. Normalized developmental time courses for global form and motion sensitivity. The same data sets as in Fig. 3 are plotted normalized to adult values for each pattern type. Linear form and translational motion sensitivity are plotted together in panel A; concentric form and rotational motion sensitivity are plotted together in panel B. The smooth curves are fits to the data sets (denoted by color), which capture the developmental trends (see Section 2.3). The colored open circles and horizontal lines along the abscissa represent computed age at half-saturation, ±1SD, for each fit.

only at relatively large dot displacements/separations. At the older test ages, she was able to discriminate patterns over a wider range of Δx values, although the sensitive range was broader for motion stimuli than for Glass patterns. Third, coherence sensitivity for all pattern types improved with age. By the second test age she was able to perform reasonably well even with linear Glass patterns (panel D, 32 weeks). Finally, her coherence sensitivity was always higher with motion stimuli than with the comparable Glass pattern type at the same test age. In other words, coherence sensitivity for rotational motion was higher than for concentric Glass patterns, and sensitivity for translational motion was higher than for linear Glass patterns. This is not likely to have been a result of "motion streaks", which can occur in high coherence RDKs (see Section 2.2), since her thresholds were near 0.2 even at this young age.

To characterize the developmental time courses for sensitivity to motion and form, we plotted the best sensitivity obtained at any Δx for each pattern type measured for each animal as a function of age (Fig. 3). The data for the two types of motion stimuli, rotation (dark gray) and translation (red), are plotted in Fig. 3A; those for the two types of Glass patterns, concentric (light gray) and linear (blue), are plotted in Fig. 3B. The downward pointing arrows represent ages at which animals were tested with the Glass pattern stimuli but failed to perform at levels above chance; open triangles represent cases that were able to perform the task above 80% correct at the highest coherence level only, but were at chance for lower coherence levels. The data are a mixture of cross-sectional and longitudinal measurements, with 19 of the 24 subjects providing multiple data points. Note that the number of data points contributed by a given animal may be different depending on the pattern type since, as represented in Fig. 2 and as revealed by the arrows and triangles in Fig. 3, the stimuli were not all successfully discriminated at all test ages by all monkeys. As shown for the individual case in Fig. 2, these population data show a slow, steady improvement in sensitivity for both patterns of motion from the earliest test ages, while sensitivity for Glass patterns emerges somewhat later. Most animals were able to detect the structure in concentric Glass patterns before they could detect linear structure. At all ages, the animals were more than twice as sensitive to motion coherence as to form coherence. Bootstrap results for sensitivity at adult levels (evaluated from the fitted values at 202 weeks, the last measurement age) showed significantly higher

sensitivity for motion than form (translational motion vs. linear Glass: $p < 0.001$; rotational motion vs. concentric Glass: $p < 0.001$); there was no significant difference between motion types ($p = 0.21$) or between form types ($p = 0.085$).

To determine whether the developmental progression is similar across the different pattern types once sensitivity becomes measurable, we normalized the data from Fig. 3 to adult levels for each pattern type. These normalized data are plotted in Fig. 4, in which we directly compare the analogous form and motion developmental progressions. Fig. 4A compares sensitivity to translational motion and linear Glass patterns; Fig. 4B compares sensitivity to rotational motion and concentric Glass patterns. The smooth function fit to each data set provides a metric for quantitative comparison across the data sets (see Section 2.3). Our benchmark for these comparisons is the age at which sensitivity reached half of the adult level. The colored open circles and associated lines along the abscissa indicate this age, along with a bootstrap estimate of the standard deviation for each data set. Analysis of these computed half-peak ages revealed no significant differences (rotation vs. concentric Glass: $p = 0.53$; translation vs. linear Glass: $p = 0.45$; see Section 2.3; El-Shamayleh, Movshon, & Kiorpes,
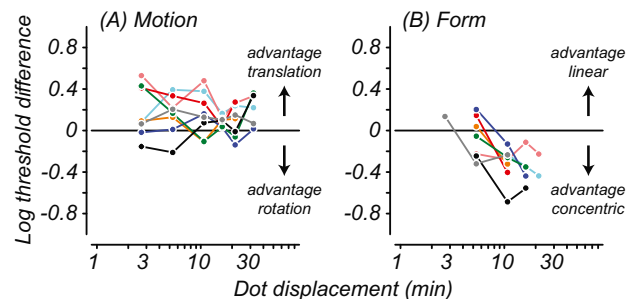
Fig. 5. Relative sensitivity to different pattern types for RDK and Glass pattern stimuli. Ratio of sensitivity (log threshold difference) between rotational and translational motion is plotted as a function of spatial scale for adult monkeys (>2 years). Individual animals' data are represented by different colors. For some animals, translational motion has a slight advantage over rotational motion (panel A), with positive ratios across Δx. All animals show an advantage of concentric Glass patterns over linear ones (negative ratios), but mainly at moderate and large Δx.
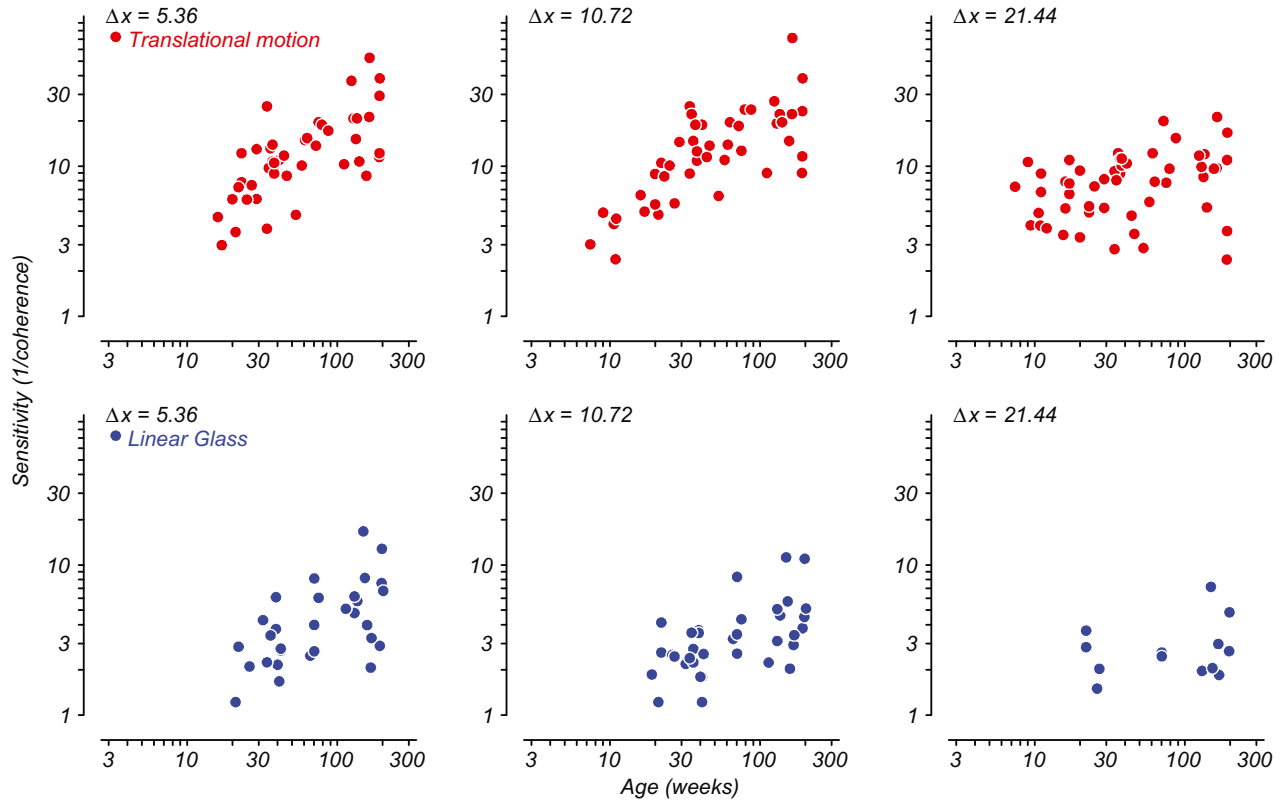
Fig. 6. Developmental profiles for parallel stimulus patterns at three spatial scales. Coherence sensitivity is plotted as a function of age for translational motion (top row) and linear form (bottom row) at three spatial scales: Δx of 5.36, 10.72, 21.44 (speed range 4.4–17.7 deg/s). Greater change in sensitivity with age is apparent for moderate and fine Δx than for large Δx.
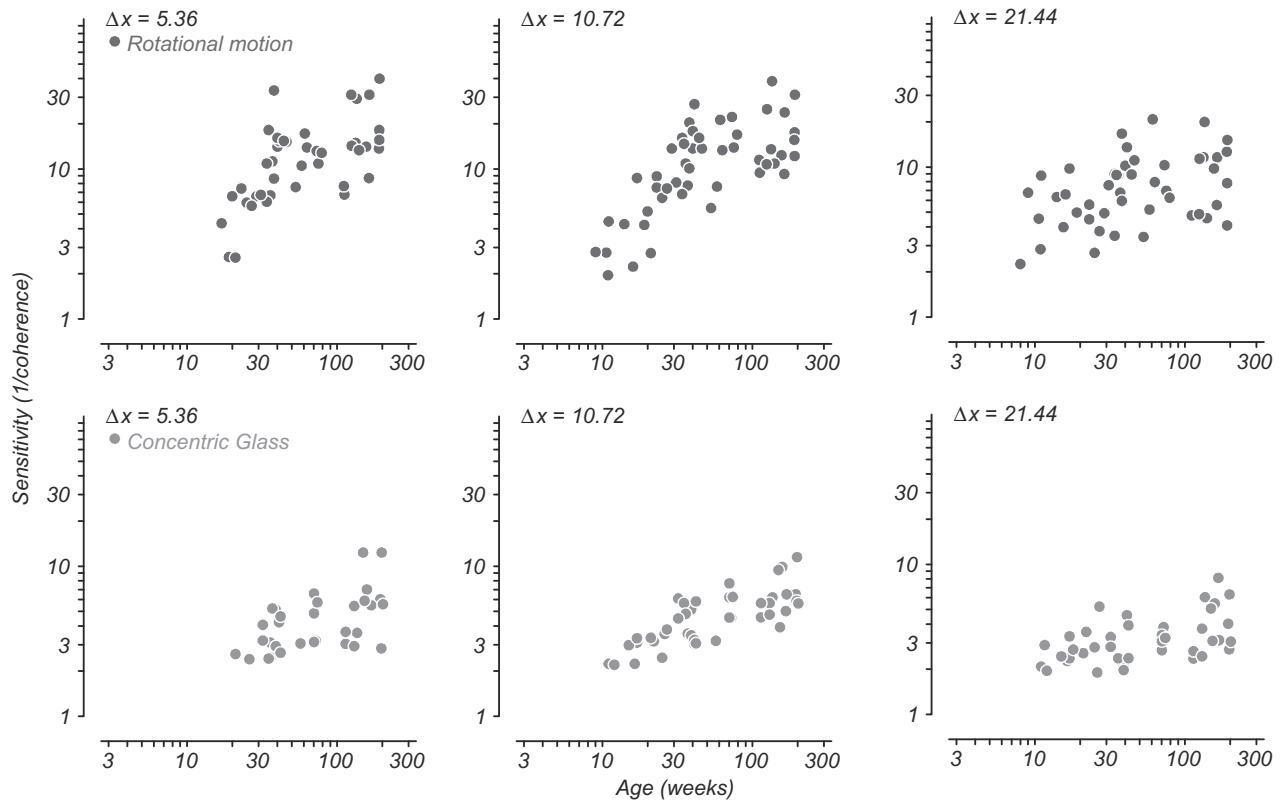
Fig. 7. Developmental profiles for circular stimulus patterns at three spatial scales. Format is the same as for Fig. 6, but for rotational motion (top row) and concentric form (bottom row).

2010), suggesting that sensitivity to RDKs and Glass patterns mature at similar rates. The range of individual variation in threshold for all pattern types is quite large, even among the adults, making it difficult to reliably quantify an "age at maturation". We therefore rely on the age at half-maximum to compare across pattern types.

Within a domain, form or motion, sensitivity to the different pattern types was not necessarily the same for a given individual. Most individuals were more sensitive to translational motion than to rotational motion, while the opposite was true in the form domain – they were often more sensitive to concentric Glass patterns than to linear ones. These sensitivity ratios for motion patterns and form patterns are shown in Fig. 5A and B, respectively, for the adult subjects (all animals older than 2 years). The relationship is fairly consistent across Δx for motion, although in some cases sensitivity is equivalent for translation and rotation. However, the superiority of sensitivity to concentric over linear Glass patterns is apparent only at moderate and large Δx, and is not consistently evident at fine dot separations.

Coherence sensitivity varies with Δx for both form and motion stimuli. The pattern changes with development, making it of interest to evaluate developmental trends at different Δx values. In an earlier study of global motion development, we found that the youngest infants were sensitive only to the largest values of Δx (fastest speeds) but the range of Δx sensitivity expanded with age to include smaller values (slower speeds) (Kiorpes & Movshon, 2004). We found a similar pattern of development here, for both form and motion stimuli. The youngest infants were able to perform the discriminations at large Δx only. As they got older, they were able to succeed at smaller Δx (refer to Fig. 2, for example). An exception was the comparatively late development of sensitivity to linear Glass patterns, which most animals were unable to discriminate at any Δx prior to 20 weeks. Developmental data for three representative Δx's are shown for each pattern type for motion and form domains in Figs. 6 and 7, respectively. Fig. 6 includes data for translational motion and linear Glass patterns; Fig. 7 includes rotational motion and concentric Glass pattern data. These figures show relatively greater development at the moderate and fine Δx's compared to the largest Δx, which is expected since sensitivity to the large Δx's is comparatively mature at young ages. We found greater overall improvement in sensitivity with age for motion than for form stimuli regardless of Δx. Finally, for each pattern type, performance was measurable earlier with motion stimuli than with Glass patterns, and linear Glass pattern discrimination was consistently late to develop.

Taken together, the data reveal generally similar time courses for maturation of form and motion sensitivity, but motion discrimination is evident earlier and develops to a greater degree than form discrimination (see Fig. 4). One possible explanation for the earlier development of motion sensitivity is an "iceberg" effect, due to the overall lower sensitivity to Glass patterns compared to RDKs, even in adults. Suppose that sensitivity to global stimuli of both kinds is limited by the same factors, but sensitivity is higher to moving than static stimuli. During maturation, motion stimuli would be detectable earlier than comparable static ones. If the lag in form sensitivity is simply due to such an "iceberg" effect, then we would expect to find a consistent sensitivity ratio across age for a comparable set of stimuli. To evaluate this possibility, we computed the sensitivity ratio for comparable form and motion stimuli as a function of age, for a given Δx. The comparisons, plotted in Fig. 8 for one moderate Δx, do not robustly support for this idea. Fig. 8 A and B show the ratio of sensitivity between "linear" pattern types (translational motion and linear form), and "circular" ones (rotational motion and concentric form), for individual animals as a function of age. The plots include data only from individuals for which we obtained thresholds with each pattern type at
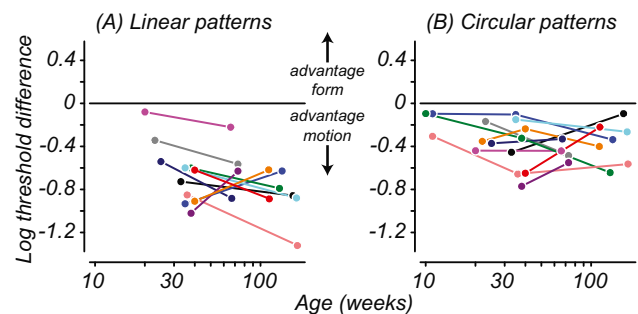
Fig. 8. Relative sensitivity between form and motion stimuli for analogous patterns at a single Δx (10.72 min; 8.9 deg/s). Ratio of sensitivity (log threshold difference) between linear pattern types (A, translation; linear Glass) and between circular pattern types (B, rotation; concentric Glass) form and motion plotted as a function of age. Colored symbols and lines represent data from individual animals (colors are matched to those in Fig. 5 for animals whose data appear in both figures). Data are included for animals that had measurable thresholds for at least two ages for each pattern type ($n = 11$). The sensitivity advantage for motion stimuli is much greater for linear/translational patterns compared with concentric/rotational ones and increases with age.

two or more ages. While there is variability across individuals, there is an overall increase in sensitivity ratio with age for linear patterns (Fig. 8A, $r = -0.46$, $p = 0.03$); for circular patterns this trend is not evident (Fig. 8B, $r = -0.29$, $p = 0.13$).

4. Discussion

As described in Section 1, there is no clear consensus regarding relative developmental time courses for global form and motion sensitivity. The present study is the first longitudinal comparison of these functions. Using comparable stimuli to test the two domains, we found evidence for perception of global motion earlier than global form, but thereafter the developmental profiles were generally similar, meaning that both functions approach adult levels at about the same rate. Our results were obtained with analogous form and motion stimuli, suggesting that conflicting results in the human literature, described earlier (Section 1), may well be due to differences in the stimuli or measures used to test form and motion sensitivity (see Braddick, Atkinson, & Wattam-Bell, 2003; Parrish et al., 2005).

In addition to the age at maturation, we found similar developmental shifts in spatial scale tuning for global form and motion. The youngest animals were most sensitive to the largest displacements (Δx), which is reminiscent of our previous findings for global motion direction discrimination (Kiorpes & Movshon, 2004). This shift in scale sensitivity across age is not due to the change in viewing distance or other stimulus parameters for animals tested initially with the reinforced looking technique and later with independent operant testing. As noted above (Section 2.3), we compared data collected under the different test paradigms in several individual animals; we did not find systematic differences across test methods, either in best sensitivity or best Δx. Furthermore, there is no obvious break in the developmental trends in the transition age range (around 6 months), as might be expected if the change in test methods affected the measured thresholds. The greatest overall change in sensitivity with age was in the mid- and fine-displacement ranges for both Glass patterns and RDKs (Fig. 6 and 7). This is an important point because most studies of human infants and children test one spatial scale or dot speed. The developmental profile obtained will depend on what displacement or speed values are chosen (see also, Ellemberg et al., 2004; Haywood et al., 2011; Hou et al., 2009).

While the overall trends for form and motion development are similar, their onset as measured by coherence sensitivity was not coincident and depended on the pattern type. In all animals, global motion stimuli of both types were perceived at the earliest test ages (<11 weeks). However, Glass patterns were not detectable by most animals before 15–20 weeks. In virtually every case, concentric Glass patterns were detectable before linear ones. These distinctions largely reflect differences in sensitivity between these patterns in adults. In adult monkeys, sensitivity is higher for concentric patterns than linear ones (Fig. 5). Poor sensitivity for linear Glass patterns is consistent with most data from human adults (Wilson, Wilkinson, & Asaad, 1997; see also Rislove et al., 2010). The existence of the developmental distinction supports the notion that there is a fundamental difference in the way that linear patterns are processed by the visual system.

There is wide acceptance of the idea that sensitivity to global motion reflects the function of the dorsal visual processing stream, while sensitivity to form in Glass patterns depends on the function of the ventral stream. Our finding of earlier sensitivity to global motion than global form stimuli is consistent with physiological and anatomical data showing earlier development of dorsal than ventral stream areas in macaques. Using the visually evoked uptake of $C^{14}2$-deoxyglucose, Distler and colleagues studied the relative development of extrastriate areas in the macaque and found that extrastriate area MT, in the dorsal stream, matured earlier than areas in the ventral stream (Distler et al., 1996). Using specific neuronal markers, several studies have reported earlier maturation of dorsal stream than other extrastriate areas (Bourne & Rosa, 2006; Condé, Lund, & Lewis, 1996). Neurophysiological recordings from area MT of monkeys as young as 1 week old revealed active directionally-selective neurons tuned similarly to those in adults but somewhat less responsive (Movshon et al., 2004). Rodman, Scalaidhe, and Gross (1993) recorded from single neurons in MT and IT and found that MT neurons were responsive earlier than those in IT. Consistent with these findings in nonhuman primates, one high-density VERP study in human infants found global motion responses to be more prevalent in 4 month olds than global form responses, although the activation patterns were different in infants compared to adults (Wattam-Bell et al., 2010). Therefore, the balance of evidence suggests that dorsal stream function is evident before ventral stream.

It is unclear, then, why dorsal stream function appears to be more compromised than ventral stream function in many cases of atypical development (see, e.g., Braddick, Atkinson, & Wattam-Bell, 2003; Spencer et al., 2000; Taylor et al., 2009). Since many of the disorders studied have a genetic component (Williams Syndrome, Autism) or are related to very premature birth, one could imagine that critical connectivity forming prenatally may be more susceptible to insult than later developing pathways in these cases. If this were so, then dorsal stream could be more vulnerable due to earlier rather than later development. Consistent with this idea, Burkhalter and colleagues described later, protracted postnatal development of local, intracortical circuits and intercortical feedback connections for pathways that subserve ventral stream function in humans (Burkhalter, 1993; Burkhalter, Bernardo, & Charles, 1993).

Because of our finding that the *rates* of developmental progress are similar for form and motion (Figs. 4, 6 and 7), we considered the possibility that the earlier development of motion sensitivity reflects an "iceberg" effect related to the fact that motion is processed more efficiently, earlier than form in these random-dot stimuli. This account is incomplete, at least for linear pattern types, because the relationship between form and motion thresholds changes with age (Fig. 8). Rather, since the primate visual system is most sensitive to moving stimuli in general, which has a distinct evolutionary advantage, we suggest that there is an earlier developmental onset for stimuli for which there is high sensitivity and value to the organism.

5. Conclusions

In conclusion, we find earlier perception of global motion patterns compared to global form, consistent with anatomical and physiological data suggesting earlier postnatal maturation of the dorsal than ventral cortical pathways. However, beyond the earliest time points, these global visual functions proceed apace and approach maturity at a similar age, which in the macaque monkey is near the end of the second postnatal year. The convergence of age at maturation for these global visual functions, and others we have documented (Hall-Haro & Kiorpes, 2008; Kiorpes & Bassin, 2003), may reflect a more general end to the developmental program for the extrastriate visual system.

Acknowledgments

References

Alliston, E. L. (2004). *Glass patterns and random dot motion: Parallel and hierarchical visual processing.* PhD dissertation. New York University. <http://wwwlib.umi.com/dissertations/fullcit/3127423>.

Altmann, C. F., Bülthoff, H. H., & Kourtzi, Z. (2003). Perceptual organization of local elements into global shapes in the human visual cortex. *Current Biology, 13*(4), 342–349.

Arcand, C., Tremblay, E., Vannasing, P., Ouimet, C., Roy, M. S., Fallaha, N., et al. (2007). Development of visual texture segregation during the first year of life: A high-density electrophysiological study. *Experimental Brain Research, 180*(2), 263–272.

Atkinson, J., & Braddick, O. (1992). Visual segmentation of oriented textures by infants. *Behavioural Brain Research, 49*, 123–131.

Boothe, R. G., Kiorpes, L., Williams, R. A., & Teller, D. Y. (1988). Operant measurements of contrast sensitivity in infant macaque monkeys during normal development. *Vision Research, 28*(3), 387–396.

Bourne, J. A., & Rosa, M. G. (2006). Hierarchical development of the primate visual cortex, as revealed by neurofilament immunoreactivity: Early maturation of the middle temporal area (MT). *Cerebral Cortex, 16*(3), 405–414.

Braddick, O., Atkinson, J., & Wattam-Bell, J. (2003). Normal and anomalous development of visual motion processing: Motion coherence and 'dorsal stream vulnerability'. *Neuropsychologia, 41*, 1769–1784.

Braddick, O., Birtles, D., Wattam-Bell, J., & Atkinson, J. (2005). Motion- and orientation-specific cortical responses in infancy. *Vision Research, 45*, 3169–3179.

Britten, K. H., Shadlen, M. N., Newsome, W. T., & Movshon, J. A. (1992). The analysis of visual motion: A comparison of neuronal and psychophysical performance. *Journal of Neuroscience, 12*, 4745–4765.

Britten, K. H., Shadlen, M. N., Newsome, W. T., & Movshon, J. A. (1993). Responses of neurons in macaque MT to stochastic motion signals. *Visual Neuroscience, 10*, 1157–1169.

Bucher, K., Dietrich, T., Marcar, V. L., Brem, S., Halder, P., Boujraf, S., et al. (2006). Maturation of luminance- and motion-defined form perception beyond adolescence: A combined ERP and fMRI study. *Neuroimage, 31*(4), 1625–1636.

Burkhalter, A. (1993). Development of forward and feedback connections between areas V1 and V2 of human visual cortex. *Cerebral Cortex, 3*(5), 476–487.

Burkhalter, A., Bernardo, K. L., & Charles, V. (1993). Development of local circuits in human visual cortex. *Journal of Neuroscience, 13*(5), 1916–1931.

Condé, F., Lund, J. S., & Lewis, D. A. (1996). The hierarchical development of monkey visual cortical regions as revealed by the maturation of parvalbumin-immunoreactive neurons. *Developmental Brain Research, 96*, 261–276.

De Weerd, P., Desimone, R., & Ungerleider, L. G. (1996). Cue-dependent deficits in grating orientation discrimination after V4 lesions in macaques. *Visual Neuroscience, 13*, 529–538.

Distler, C., Bachevalier, J., Kennedy, C., Mishkin, M., & Ungerleider, L. G. (1996). Functional development of the corticocortical pathway for motion analysis in the macaque monkey: A 14C-2-deoxyglucose study. *Cerebral Cortex, 6*, 184–195.

Downing, C. J., & Movshon, J. A. (1989). Spatial and temporal summation in the detection of motion in stochastic random dot displays. *Investigative Ophthalmology and Visual Science Supplement, 30*, 72.

Ellemberg, D., Lewis, T. L., Dirks, M., Maurer, D., Guillemot, J. P., & Lepore, F. (2004). Putting order into the development of sensitivity to global. *Vision Research, 44*, 2403–2411.

Ellemberg, D., Lewis, T. L., Liu, C. H., & Maurer, D. (1999). Development of spatial and temporal vision during childhood. *Vision Research, 39*, 2325–2333.

Ellemberg, D., Lewis, T. L., Meghji, K. S., Maurer, D., Guillemot, J. P., & Lepore, F. (2003). Comparison of sensitivity to first- and second-order local motion in 5-year-olds and adults. *Spatial Vision, 16*, 419–428.

El-Shamayleh, Y., Movshon, J. A., & Kiorpes, L. (2010). Development of sensitivity to visual texture modulation in macaque monkeys. *Journal of Vision, 10*, 1–12.

Finney, D. J. (1971). *Probit analysis*. New York: Cambridge University Press.

Gerhardstein, P., Kovacs, I., Ditre, J., & Feher, A. (2004). Detection of contour continuity and closure in three-month-olds. *Vision Research, 44*, 2981–2988.

Giaschi, D., & Regan, D. (1997). Development of motion-defined figure-ground segregation in preschool and older children, using a letter-identification task. *Optometry and Vision Science, 74*, 761–767.

Glass, L. (1969). Moire effect from random dots. *Nature, 223*(5206), 578–580.

Glass, L., & Perez, R. (1973). Perception of random dot interference patterns. *Nature, 246*(5432), 360–362.

Gunn, A., Cory, E., Atkinson, J., Braddick, O., Wattam-Bell, J., Guzzetta, A., et al. (2002). Dorsal and ventral stream sensitivity in normal development and hemiplegia. *Neuroreport, 13*, 843–847.

Hall-Haro, C., & Kiorpes, L. (2008). Normal development of pattern motion sensitivity in macaque monkeys. *Visual Neuroscience, 25*, 675–684.

Haywood, J., Truong, G., Partanen, M., & Giaschi, D. (2011). Effects of speed, age, and amblyopia on the perception of motion-defined form. *Vision Research, 51*, 2216–2223.

Hou, C., Gilmore, R. O., Pettet, M. W., & Norcia, A. M. (2009). Spatio-temporal tuning of coherent motion evoked responses in 4–6 month old infants and adults. *Vision Research, 49*, 2509–2517.

Huxlin, K. R., Saunders, R. C., Marchionini, D., Pham, H. A., & Merigan, W. H. (2000). Perceptual deficits after lesions of inferotemporal cortex in macaques. *Cerebral Cortex, 10*, 671–683.

Kiorpes, L. (1992). The development of vernier acuity and grating acuity in normally-reared monkeys. *Visual Neuroscience, 9*, 243–251.

Kiorpes, L. (2008). Macaque models of visual development and disability. In T. M. Burbacher, G. P. Sackett, & K. S. Grant (Eds.), *Nonhuman primate models of children's health and developmental disabilities* (pp. 45–70). New York: Academic Press.

Kiorpes, L., & Bassin, S. A. (2003). Development of contour integration in macaque monkeys. *Visual Neuroscience, 20*, 567–575.

Kiorpes, L., & Kiper, D. C. (1996). Development of contrast sensitivity across the visual field in macaque monkeys (*Macaca nemestrina*). *Vision Research, 36*, 239–247.

Kiorpes, L., & Movshon, J. A. (1998). Peripheral and central factors limiting the development of contrast sensitivity in macaque monkeys. *Vision Research, 38*, 61–70.

Kiorpes, L., & Movshon, J. A. (2004). Development of sensitivity to visual motion in macaque monkeys. *Visual Neuroscience, 21*, 851–859.

Kourtzi, Z., Tolias, A. S., Altmann, C. F., Augath, M., & Logothetis, N. K. (2003). Integration of local features into global shapes: Monkey and human FMRI studies. *Neuron, 37*, 333–346.

Kovács, I. (2000). Human development of perceptual organization. *Vision Research, 40*, 1301–1310.

Kovács, I., Kozma, P., Fehér, Á., & Benedek, G. (1999). Late maturation of visual spatial integration in humans. *Proceedings of the National Academy of Sciences USA, 96*, 12204–12209.

Larsson, J., Landy, M. S., & Heeger, D. J. (2006). Orientation-selective adaptation to first- and second-order patterns in human visual cortex. *Journal of Neurophysiology, 95*, 862–881.

Li, W., Piëch, V., & Gilbert, C. D. (2006). Contour saliency in primary visual cortex. *Neuron, 50*, 951–962.

Li, W., Piëch, V., & Gilbert, C. D. (2008). Learning to link visual contours. *Neuron, 57*, 442–451.

Merigan, W. H. (2000). Cortical area V4 is critical for certain texture discriminations, but this effect is not dependent on attention. *Visual Neuroscience, 17*, 949–958.

Movshon, J. A., Rust, N. C., Kohn, A., Kiorpes, L., & Hawken, M. J. (2004). Receptive field properties of MT neurons in infant macaques. *Perception, 33S*, 27.

Newsome, W. T., & Paré, E. B. (1988). A selective impairment of motion perception following lesions of the middle temporal visual area (MT). *Journal of Neuroscience, 8*(6), 2201–2211.

Norcia, A. M., Pei, F., Bonneh, Y., Hou, C., Sampath, V., & Pettet, M. W. (2005). Development of sensitivity to texture and contour information in the human infant. *Journal of Cognitive Neuroscience, 17*, 569–579.

Ostwald, D., Lam, J. M., Li, S., & Kourtzi, Z. (2008). Neural coding of global form in the human visual cortex. *Journal of Neurophysiology, 99*, 2456–2469.

Palomares, M., Pettet, M., Vildavski, V., Hou, C., & Norcia, A. (2010). Connecting the dots: How local structure affects global integration in infants. *Journal of Cognitive Neuroscience, 22*, 1557–1569.

Parrish, E. E., Giaschi, D. E., Boden, C., & Dougherty, R. (2005). The maturation of form and motion perception in school age children. *Vision Research, 45*, 827–837.

Pei, F., Pettet, M. W., & Norcia, A. M. (2007). Sensitivity and configuration-specificity of orientation-defined texture processing in infants and adults. *Vision Research, 47*, 338–348.

Rislove, E. M., Hall, E. C., Stavros, K. A., & Kiorpes, L. (2010). Scale dependent loss of global form perception in strabismic amblyopia. *Journal of Vision, 10*, 1–13.

Rodman, H. R., Scalaidhe, S. P., & Gross, C. G. (1993). Response properties of neurons in temporal cortical visual areas of infant monkeys. *Journal of Neurophysiology, 70*, 1115–1136.

Sireteanu, R., & Rieth, C. (1992). Texture segregation in infants and children. *Behavioural Brain Research, 49*, 133–139.

Spencer, J., O'Brien, J., Riggs, K., Braddick, O., Atkinson, J., & Wattam-Bell, J. (2000). Motion processing in autism: Evidence for a dorsal stream deficiency. *Neuroreport, 11*(12), 2765–2767.

Stavros, K. A., & Kiorpes, L. (2008). Behavioral measurements of temporal contrast sensitivity development in macaque monkeys (*Macaca nemestrina*). *Vision Research, 48*, 1335–1344.

Taylor, N. M., Jakobson, L. S., Maurer, D., & Lewis, T. L. (2009). Differential vulnerability of global motion, global form, and biological motion processing in full-term and pre-term children. *Neuropsychologia, 47*(13), 2766–2778.

Teller, D. Y. (1997). First glances: The vision of infants. *Investigative Ophthalmology and Visual Science, 38*, 2183–2203.

Ungerleider, L. G., & Pasternak, T. (2004). Ventral and dorsal cortical processing streams. In L. M. Chalupa, & J. S. Werner, (Eds.), *The visual neurosciences* (pp. 541–562). Cambridge: MIT Press.

Wattam-Bell, J., Birtles, D., Nystrom, P., von Hofsten, C., Rosander, K., Anker, S., et al. (2010). Reorganization of global form and motion processing during human visual development. *Current Biology, 20*, 411–415.

Wilson, H. R., Wilkinson, F., & Asaad, W. (1997). Concentric orientation summation in human form vision. *Vision Research, 37*, 2325–2330.